

To Measure In-plane conductivity of Nafion membrane with general electrochemical approach

Jian-Wei Guo^{1*}, Jian-Long Wang^{1*} Shang-kun Jiang² Li Li^{2*}

1. *Institute of Nuclear and New Energy Technology, Tsinghua University, Beijing, 100084,*

China

2. School of Chemistry and Chemical Engineering, Chongqing University, Chongqing

400044, China

* Corresponding author: E-mail address: jwguo@mail.tsinghua.edu.cn,

wangjl@mail.tsinghua.edu.cn, liliracial@cqu.edu.cn

Tel.: +86 1080194009; Fax: +86 1080194009

Highlight:

- The equivalent circuit is key for electrochemical measurements and analysis
- Our equivalent circuit was validated by both EIS and CV measurements.
- Our equivalent circuit has good in situ characterization for measuring system
- The circuit elements revealed kinetic relationship for contact resistance, in-plane conductivity, active and inactive proton in membrane

Abstract

It is important to measure in-plane conductivity of Nafion membrane for fuel cell, but this target is generally inhibited by measuring system with heterogeneous interfaces and immature electrochemical measurements. This paper simply used water media to establish stable measuring system with metal electrode and Nafion membrane, representing system as equivalent circuit. Our equivalent circuit was validated by both cyclic voltammetry (CV) and electrochemical impedance spectroscopy (EIS) measurements, also clarified connection and difference in two measurements. This electrochemistry breakthrough helps realize measuring system completely and reliably even under successive temperature cycles, providing circuit elements for kinetic analysis in contact resistance, in-plane conductivity, inactive and active proton. We also clarified that the inactive and active proton shift can dictate low frequency inductance, which is an important sign for active and stable operation in fuel cell, secondary battery and materials. All these results can induce enormous progress in multi-disciplines, making our work have great significance and broad impact for future studies.

Keywords: Nafion membrane; Direct Current; Electrochemical Impedance Spectroscopy(EIS); proton conductivity; contact interface, equivalent circuit

1. INTRODUCTION

Nafion membrane is a proton-conducting polymer, with main chain of $-\text{CF}_2-$ segments and side chain of HSO_3^- group. Since the HSO_3^- group can transport proton ($\text{H}^+\cdot\text{H}_2\text{O}$) in water media, the Nafion membrane is core material in polymer exchange membrane fuel cells and electrolysis cells^[1-3]. Therefore, it has great motivation to measure Nafion membrane conductivity, whose proton transport behavior can guide material and cell progress significantly^[4-10].

Generally, the Nafion membrane is a 2D (2-Dimension) material with large plane (cm scale) and thin thickness (10-100 μm), thus it may have anisotropic conductivity either along plane (in-plane) or along perpendicular direction (through-plane). Both conductivities are important for fuel cell, but it is difficult to measure through-plane conductivity due to measurement sensitivity in thickness direction^[11-19]. Even so, it is still important to measure the in-plane conductivity, helping develop large cell and providing characterization frequency for cell operation. Nevertheless, there are many problems to obtain reliable in-plane conductivity for Nafion membrane due to following restrictions. Firstly, the in-plane conductivity is mainly affected by many internal properties of membrane, including membrane thickness, ion exchange capacity, water uptake and channels, gas/liquid permeability and chemical/physical stability^[20-23]. Past studied tried to measure conductivity under humidified gas condition, but they usually confront complex water-membrane balance. This operation mode lays a large difficulty to obtain stable in-plane conductivity, other than its kinetic relationship under temperature effect^[11,13,24,25].

Secondly, most studies used metal electrode to establish contact interfaces with membrane, thus composing of measuring system with metal electrode and membrane. Since the metal electrode and membrane transfer electron and proton, respectively, their contact interfaces must experience continuous or discontinuous flowing for heterogeneous charges. This inhibits to obtain stable membrane conductivity, presenting challenge issues in measurement [13, 17, 18,22, 26,27].

Thirdly, most studies used electrochemical measurement methods, thus both DC (Direct current) and AC (Alternative current) methods with different approaches can be used. On the one hand, the CV measurement is a typical DC method, but it can only obtain insufficient information, making it as reference measurement [15, 22,28]. On the other hand, Electrochemical Impedance Spectroscopy (EIS) is an advanced AC (Alternative current) method, and it mainly uses multi frequency to reveal measuring system completely, promising to separate electron and proton process efficiently. Unfortunately, the EIS is still immature in reliable measurement and analysis, and it often dictates complex electric responses with resistances, capacitance and inductance. In most cases, these complex electric responses are fitted with equivalent circuit, but this fitting approach usually has multi equivalent circuits, incapable to achieve effective analysis [5,6,15,28]. Consequently, the EIS is still a large obstacle to obtain reliable in-plane conductivity for Nafion membrane, requiring its core breakthrough in electrochemistry.

To address above issues, this paper simply selects water media as operation condition, which can hydrate Nafion membrane sufficiently and ignore particular properties of

membrane. Furthermore, this simple water condition helps membrane and metal electrodes to establish stable measuring system, representing as equivalent circuit. With a core idea in electrochemistry, Scheme 1 proposed that the equivalent circuit dictates various electric responses in CV and EIS measurements, and the equivalent circuit is the bridge for two measurements ^[29]. Therefore, the equivalent circuit helps differentiate and connect two measurements, playing a key role to clarify electron and proton process in the measuring system. Undoubtedly, this clarification can obtain complete and reliable circuit elements, helping reveal kinetic relationship for measuring system under successive temperature cycles. This will drive in situ characterization for in-plane conductance of membrane, thus inducing significant progress for materials and cells simultaneously.

2. EXPERIMENTAL SECTIONS

2.1 Materials and preparation

The ultrapure water with high electrical resistivity at 18Mohm cm (conductivity at 0.055 μ S/cm) was used in whole experiments. All glasswares were immersed into concentrated nitric acid to remove any residues for more than 24 hrs, and then they were cleaned in boiling water for more than six times.

The Nafion XL-100 membrane (DuPont, thickness of 27.5 μ m) was used as standard sample, which can be prepared for fuel cell directly according to supplier's specification. Therefore, we just immersed the Nafion XL-100 membrane into ultrapure water before one-day measurement, helping attain its sufficient hydration state.

2.2 Measuring electrode and Fixture

To illustrate in-plane conductivity measurement, Fig.1 a exhibits measuring electrodes as Pt lines, with small diameter ($\Phi=0.5\text{mm}$) towards exact measurement ^[13]. Figure 1b shows the measuring fixture with Nafion membrane, and the fixture was made by insulative PTFE materials with same top and bottom segments. In its middle section, the fixture has blank area to permit water transfer freely. On its opposite edges, the fixture has inner grooves to fasten Pt lines, with 1cm distance for adjacent lines.

2.3 Membrane Installation and operation

To install membrane in fixture (Figure 1b), the Nafion membrane was put on bottom segment of fixture, and its top surface was attached on four parallel Pt wires fastened by insulative tapes. Then, the top segment of fixture was covered on membrane, and the whole fixture was fastened by PTFE screws under torque of 1.5 N m . Subsequently, the whole fixture was immersed into ultrapure water bath covered by protection membrane. Finally, the fixture in ultrapure water bath was put into heating water bath, whose temperature was controlled to increase from 20 to 100°C in every day. Each temperature was kept at least 20 minutes for stability before measurement, and the whole measurement processes were carried out on 3 days successively.

2.4 The in-plane conductivity measurement for Nafion Membrane

The electrochemical measurement was carried on Solartron EnergyLab workstation,

with specific definition as RE₁, RE₂ corresponding to reference electrode (RE) and sensor electrode(SE), respectively. According to principle for 4-electrode measurement, the RE and SE were used to control potential as outside lines, while counter electrode (CE) and working electrode(WE) were used to reflect current as inside lines [25]. Figure 1c shows the 4-electrode composition as RE₁(RE)-CE-WE-RE₂(SE), with 1cm distance (d) for adjacent lines. Figure 1c also labelled membrane length (w= 5cm) and thickness (t= 27.5 μm), helping calculate in-plane conductivity.

We adopted cyclic voltammetry (CV) and EIS measurements under potential mode, corresponding to DC and AC measurement methods, respectively. On CV measurement, the potential was set as 0-1V range with scan rate of 20 mV/s. On EIS measurement, the frequency range was set as 1M Hz ~1m Hz, with amplitude of sinusoidal potential at 10 mV but without any DC potential deviation. With Zview software, the measured EIS dates were checked reliability under Kramers-Kronig transformation, and then they were fitted with equivalent circuit. Furthermore, the in-plane conductivity (σ , S cm⁻¹) of Nafion membrane was calculated as :

$$\sigma = \frac{d}{w \cdot t \cdot R}$$

Where, d is current line distance (1cm) between CE-WE, w and t are membrane length(5cm) and thickness (27.5 μm), and R is resistance (ohm) in EIS measurement.

3. RESULTS AND DISCUSSIONS

3.1 Basic features for CV and EIS measurement

To understand basic measurements, Fig. 2 illustrates typical CV and EIS results at 30

°C condition in 1st day. Fig. 2(a) shows that the CV under potential range of 0-1V can induce ~0.2-1.2 mA with a straight and reversible line, dominated by resistance at 1037.3ohm. This can be due to total resistance from electron and proton with successive transportation, thus dictating Ohm's law as Equation(1)

$$\eta_{ohmic}^{total} = \eta_{ohmic}^{electronic} + \eta_{ohmic}^{protons} = -i R^{interal} \quad (1)$$

In the meanwhile, the membrane conductivity (K) is determined as Equation(2):

$$K = F^2 D_{H^+} C_{H^+} / RT \quad (2)$$

where, F is Faraday's constant(96,487 C/mol), R is gas constant, 8.3143 J/(mol)(K). T is Kelvin temperature, C_{H^+} , D_{H^+} are concentration and diffusivity of H⁺ species (H⁺•H₂O), respectively.

Since the C_{H^+} , D_{H^+} are dependent upon the water content and distribution in the membrane, the proton conductivity and resistance are constant^[30]. Therefore, this simple CV measurement can provide resistance information, dictating Ohm's law in the heterogeneous system.

Fig. 2(b) further shows EIS measurement, whose Nyquist plot exhibits high frequency arc for capacitance (HF, 1000 K-2~6K Hz) at 1st quadrant, in contrast to low frequency (LF, 2~6 K- 0.3Hz) arc for inductance at 4th quadrant. From the view of electricity, the capacitance always help proton mobility but the inductance always inhibit proton mobility. Therefore, it is explicit that the intersection point at abscissa axis is the maximum of proton mobility, corresponding to membrane resistance at 1365.5ohm. These two opposing phenomena can be due to opposing proton behaviors on Nafion membrane. On the one hand, the proton mainly transport through water channels in

membrane, dictating as proton mobility. On the other hand, the HSO_3^- group in membrane has strong interaction with proton, thus inhibiting proton mobility to dictate mobility hysteresis behavior [22,31]. This clarification is very important to realize the proton mobility in Nafion membrane, thus having a general theoretical significance.

It should be stressed that this LF loop is a common feature in fuel cell operation, but this has been largely shielded due to complex cell operation [32,33]. Past studies found that the LF inductive is mainly related to slow kinetics for Nafion ionomer humidification[34], along with ionomer swelling/shrinking (hydration/dehydration) cycles in cathode catalyst layer [35--37]. Only recently, the high-frequency resistance measurement can capture the ohmic resistance accurately, corresponding to the frequency of zero-phase from 1 kHz -10 kHz [38]. This frequency range(1-10K Hz) strongly supporting 2-6K Hz in our approach, indicating it as a characterization frequency for humidified Nafion membrane. Therefore, our EIS measurement can obtain more information than that in CV measurement, penetrating into membrane structure insightfully.

3.2 Equivalent circuit buildup

Fig. 3a depicts that both DC and AC measurements can induce main response on contact interface (Pt electrodes and Nafion membrane) and Nafion membrane, inevitably dictating as Equivalent circuit. Fig. 3b proposed that the contact interfaces transfer heterogeneous charges, probably establishing parallel circuit for contact capacitor (C_0) and contact resistance (R_0) [39]. Fortunately, Fig.2b shows the high

frequency(HF) comes from original point if extrapolating high frequency linearly, indicating low contact resistance (R_0). This also means the higher frequency can drive quick charging/discharging process for contact capacitor (C_0), thus the contact capacitor can attain steady state to present low contact resistance (R_0). Therefore, Fig.3b only keeps contact resistance (R_0), without considering contact capacitor presence. Moreover, Fig.3a proposes the electric field (U) on membrane can establish three parallel processes in Fig.3b.

1st, The electric field establishes charge reservoir, similar as capacitor to keep heterogeneous charges in membrane. Considering leakage current between measuring electrodes, Fig.3b used constant phase element (CPE) to represent capacitor.

2nd, The electric field can drive active proton mobility in water channels, presenting proton resistance (R_1).

3rd, The electric field cannot drive inactive proton mobility in HSO_3^- group. Since this dictates proton mobility hysteresis in LF region, Fig.3b uses series path of R_2 - L_2 to represent inactive resistance and inductance.

Therefore, Fig. 3b proposes equivalent circuit with explicit physical meanings for all elements, helping check various measurements.

3.3 Validation of the Equivalent circuit

After successive measurements, we checked all EIS data reliability and then fitted them with equivalent circuit. Fig 4 only exhibits the measured and fitted Nyquist spectrums in 1st day, illustrating their high fitting manners. Table 1-3 further lists all

fitted parameters under successive temperature cycles in 3 days, showing fitting with total Chi-square errors less than 0.4253. These results support the equivalent circuit is effective to reflect EIS measurement, helping reveal measuring system completely and dynamically.

As a typical DC approach, the CV measurement experiences open path for capacitance and short path for inductance in the equivalent circuit. Therefore, the steady CV measurement only makes total resistance response in equivalent circuit, dictating as $R_0 + R_1R_2/(R_1+R_2)$. Fig.5 compares the measured resistance in CV measurement and the fitted resistance of $R_0 + R_1R_2/(R_1+R_2)$ in EIS measurement (Table 1-3), indicating their high similarity even under successive temperature cycles. This similarity not only makes inter-corroboration for two measurement, but also validates general effectiveness for equivalent circuit.

With its bridge role, the equivalent circuit should differentiate CV and EIS response. As shown before, the steady CV measurement makes total resistance response as $R_0 + R_1R_2/(R_1+R_2)$. From equivalent circuit, the parallel resistance for R_1 and R_2 is smaller than individual resistance, leading to $R_0 + R_1R_2/(R_1+R_2) < R_0 + R_1$. Noticeably, Table (1-3) show all R_0 values are smaller than other resistances, suggesting $R_0 + R_1R_2/(R_1+R_2) \leq R_1$. This general relationship can be found in Fig. 2, where the $R_0 + R_1R_2/(R_1+R_2)$ resistance at 1037.3 ohm in CV measurement is smaller than R_1 resistance at 1365.5ohm in EIS measurement.

The above clarification supports that the CV measurement has total resistance response, driving both inactive and active proton transportation in equivalent circuit. Furthermore,

the Ohm's law can apply for measuring system with heterogeneous interface, extending the traditional Ohm's law range in metal system with good electron conductivity. Moreover, the above clarification makes explicit that the EIS measurement mainly use multi frequency to reveal various electric responses, helping obtain equivalent circuit directly. Consequently, both CV and EIS measurement can support reliable equivalent circuit with inter-corroboration, helping reflect measuring system completely and dynamically. This general electrochemistry approach helps reveal kinetic physical-chemistry process in measuring system, thus providing In Situ characterization technique insightfully.

3.4 The circuit elements analysis for kinetic relationship.

3.4.1 The contact resistance

Based on equivalent circuit validity, the circuit element can disclose measuring system under dynamical operation. Fig 6 demonstrates the contact resistance (R_0) has small values of -20-40 ohm, indicating tight contact interface (Pt wire/membrane) under successive temperature cycles. Fig 6 further shows the R_0 fluctuated largely below 80 °C but kept stable after 80 °C, indicating challenge interface change.

Generally, the Nafion membrane has glass transition temperatures (T_g) at 80 ~ 85 °C, where the main- and side-chains of membrane occur long-range mobility. This mobility may last at 110 °C, dictating as α -relaxation process[31]. Furthermore, the Nafion membrane has high swelling ratio above 80°C, and its dimension usually changes in the through-plane direction. This helps tight membrane towards measuring

electrodes, thus keeping steady contact resistance (R_0) [24]. In contrast, past studies found in the cooling run, the membrane may occur β -relaxation process towards main-chain motions at 35 °C, and this β -relaxation process should relief stress at 70–75 °C in the following heating run [40]. Therefore, in the temperature cycles below 80 °C, the membrane usually occur re-organization, thus its unstable swelling ratio can dictate significant fluctuation for contact resistance (R_0). Consequently, our kinetic relationship for contact resistance provides dynamical characterization for hard electrode-soft membrane, relating with advanced characterizations strongly.

3.4.2 The CPE on membrane

Under successive EIS measurement, the electric field on membrane can be revealed by constant phase element (CPE) with resistance $Z_Q = \frac{1}{Y_0} (j\omega)^{-n}$, where Y_0 is reflection signal and “n” can index special process. Table 1-3 show all CPE-n lie in 0.89-0.99, indicating rough or porous membrane to establish ideal capacitor ($n=1$) [41]. This further suggested that the electric field establishes on rough surface and porous structure in membrane, promising in situ characterization completely and dynamically.

3.4.3 The in-plane conductivity for Nafion membrane

Fig. 7 (a-c) compare the in-plane proton resistance measured at the characteristic frequency (2-6K Hz) and fitted resistance (R_1) in equivalent circuit, dictating their high similarity under successive temperature cycles. This strongly supports the characteristic frequency (2-6K Hz) is a simple tool to obtain Nafion membrane resistance, helping

fuel cell evaluation directly.

Fig.7(a-c) further exhibits the increasing temperature can decrease proton resistance while increase proton conductivity monotonically. This kinetic relationship can be realized in two aspects, Nafion membrane and water media condition. On the one hand, the membrane experience slight structure change below 80°C where β -relaxation process help membrane re-organization. When temperature is higher than 80°C, the membrane began to experience glass transition process, thus the α -relaxation process can increase internal volume and outer dimension, along with reduction of ionomer density in membrane remarkably^[24,40,42-44]. On the other hand, the increasing temperature can gradually increase water activity in water media, shifting water diffusion towards convection in operation condition.

Based on the above clarification, it can be determined that at low temperature, the water media mainly adopt Fick diffusion into membrane, whose surface and thickness can strongly inhibit water diffusion towards bulk polymer^[26,45,46]. In the meanwhile, the membrane surface is enrich of sulfonic acid ionic clusters, leading to strong surface conductivity^[23,26, 46-48].

With the temperature increasing, the water media can shift diffusion towards convection, and the membrane can decrease its pore fluid viscosity gradually. This can accelerate water transport towards bulk polymer, making conductive pathways and connectivity network smoothly^[49]. Simultaneously, the increasing temperature can reduce activation barrier for proton transportation between hydrophilic clusters of membrane, driving bulk conductivity^[3]. This case is more serious when attaining glass temperature (80°C),

where membrane can enlarge internal volume to permit more water transportation significantly. Due to above reasons, the increasing temperature can decrease proton resistance while increase proton conductivity for Nafion membrane monotonically in water media.

To provide high-standard comparison, we selected critical 80 °C condition as baseline, dictating in-plane conductivities at 0.12,0.115, 0.1 S cm⁻¹ under successive 3 days. These values are highly consistent with 0.12 S cm⁻¹ in liquid water media at 80 °C [13], driving measurement towards standardization. Fig 7 further shows the in-plane conductivities in 20 -100°C lie in 0.04-0.15 S cm⁻¹ in 1st day, 0.06-0.13 S cm⁻¹ in 2nd day, 0,06-0.118 S cm⁻¹ in 3rd day. This fluctuation can be due to that the successive temperature cycles can drive bulk polymer loss and volume change, thus adjusting conduction channels slightly [3,24,,50,51].

3.4.4 The LF loop

Under successive temperature cycles, Fig 8 exhibits the R₂ resistance and L₂ inductance fluctuation significantly, coming from low frequency (LF) loop in EIS measurement. From electrical opinion, the L₂ inductance always induces counter electromotive force under electric fluctuation, helping keep steady measurement process. In this case, only the R₂ resistance can dictate inactive proton mobility with strong interaction of sulfuric groups [3233], in contrast to R₁ resistance as active proton mobility in water channels. Furthermore, the large fluctuation of R₂ in the range of 2000-8000ohm (Fig 8) indicates that the inactive proton shifts towards active proton, thus maintaining proton mobility

effectively. Therefore, this shift helps characterize water role in membrane, usually dictating conductivity hysteresis in LF loop ^[12,52].

It should be stressed that this low frequency(LF) loop in EIS measurement is very similar to DC measurement without any frequency, making it as central issue in electrochemistry. Furthermore, the LF inductance always means some inductance can induce counter electromotive force, suggesting it is an important sign for stable system ^[53,54]. As shown before, the LF inductive is mainly related to Nafion ionomer humidification ^[34] and swelling/shrinking (hydration/dehydration) cycles, helping study the challenge tri-phase boundary in cell operation ^[35-37]. Therefore, our LF loop on Nafion membrane provides core material support for active and stable fuel cell, also helping clarify water role in cell operation.

Our LF inductance has great reference for secondary battery, in which the lead/acid battery^[55] and lithium-ion battery ^[56] reported their LF inductive on electrode/electrolyte interfaces. Furthermore, our LF inductance has great reference for various kinds of materials. For metal materials, the high-Entropy alloy and 304 stainless steel usually experience surface passivation along with pitting from aggressive Cl⁻ in NaCl solution. These pitting- passivation phenomena can be identified in LF loop, supporting stable system under activation process ^[57]. For semiconductor materials, the p-type silicon in etching process can form submonolayer oxide on surface, whose dynamical change can be monitored by LF loop ^[58]. For composite materials preparation, the montmorillonite sheets under electrolyte effect can be identified in the LF loop ^[59]. All these studies suggest the LF inductance is an important characterization

sign for stable interface/surface under dynamic interaction, thus their electric phenomena can be usually observed in cells and secondary batteries.

Conclusion

It is very important to measure in-plane conductivity of Nafion membrane for fuel cell, but this target is generally inhibited by measuring system with heterogeneous interface and immature electrochemical measurements. This paper used water media to establish stable system with metal electrode and Nafion membrane, and further representing system as equivalent circuit. Our proposed equivalent circuit is validated by both CV measurement and EIS measurement, whose connection and difference can be clarified by the equivalent circuit. Therefore, the equivalent circuit provides in situ characterization tool to reflect system completely, and the circuit elements can penetrate into special physical process kinetically. For system under successive temperature cycles, the circuit element disclose the contact resistance changes dynamically due to relaxation process in membrane. The circuit element also determines the in-plane conductivity is surface conductivity, which shifts towards bulk conductivity with the temperature increasing, strongly relating to membrane structure and water media condition. Inspiringly, the elements found the inactive proton shifts towards active proton, helping maintain proton mobility in Nafion membrane. We also clarified this shift presents in low frequency (LF) inductance, which is an important sign to study stable and active operation for fuel cell, secondary battery and various kinds of materials. Consequently, our equivalent circuit make core breakthrough to

measure in-plane conductivity of Nafion membrane, driving various measurement methods as in situ characterization tool to realize measuring system. This breakthrough can induce significant paces for multi-disciplines, thus having great significance and broad impact for future studies.

Acknowledgments. This work is supported by the National Key Research and Development Program of China (2019YFB1504503), and National Natural Science Foundation of China (50873050, 51273103, 51573084, 21776158).

References

- [1]. Guo, K.; Shi, K. M.; Guo, J. W.; et al. To drive Fe-based catalyst towards complete application in proton exchange membrane fuel cells (PEMFCs). *Electrochim. Acta* **2017**, *229*, 183-196.
- [2]. Hu, T.H.; Yin Z. S.; Guo, J. W.; et al. Synthesis of Fe nanoparticles on polyaniline covered carbon nanotubes for oxygen reduction reaction. *J. Power Sources* **2014**, *272*, 661-671.
- [3]. Mali, J.; Mazu í, P.; Paidar, M.; et al. Nafion 117 stability under conditions of PEM water electrolysis at elevated temperature and pressure. *Int. J. Hydrogen Energ.* **2016**, *2177* -2188.
- [4]. Al-Madani, G.; Kailani, M. H.; Al-Hussein, M. Test System for Through-Plane Conductivity Measurements of Hydrogen Proton Exchange Membranes. *Int. J. Electrochem. Sci.* **2015**, *10*, 6465 – 6474.
- [5]. Escorihuela, J.; Narducci, R.; Compañ, V.; et al. Proton Conductivity of Composite Polyelectrolyte Membranes with Metal-Organic Frameworks for Fuel Cell Applications. *Adv. Mater. Interfaces* **2019**, *6*, 1801146.
- [6]. Guo, J. W.; Mao, Z. Q.; Xu J. M. Studies on the electrochemical behavior of polymer electrolyte membrane fuel cell (PEMFC) by AC impedance method. *Chem. J. Chinese U.* **2003**, *24*, 1477-1481.
- [7]. Guo, J. W.; Wang J. L. The pilot application of Electrochemical Impedance spectroscopy on dynamic proton exchange membrane fuel cell. *J. Electrochemistry*. **2018**, *24*, 687-696.
- [8]. Ohira, A.; Kuroda, S.; Mohamed, H. F. M. A Study on Structural Property of Ionomer as a Model for Catalyst Layer: Relationship between Thickness and Proton Conduction for Ionomer Thin Filmon Different Substrate. *ECS*

-
- Transactions* **2013**,50 (2) ,993-1001.
- [9]. Cai,G.X.; Guo, J. W.; Wang, J. ; et al. Negative resistance for methanol electro-oxidation on platinum/carbon (Pt/C) catalyst investigated by an electrochemical impedance spectroscopy. *J. Power Sources*, **2015**,276,279-290.
- [10]. Zhang, Z.; D é silets, F.; Felice, V.; et al. On the proton conductivity of Nafion–Faujasite composite membranes for low temperature direct methanol fuel cells. *J. Power Sources* **2011**, 196, 9176–9187.
- [11]. Ma, S.; Siroma, Z.; Tanaka, H. Anisotropic Conductivity Over In-Plane and Thickness Directions in Nafion-117. *J. Electrochem. Soc.* **2006**,153(12), A2274-A2281.
- [12]. Casciola, M.; Donnadio,A.; Sassi, P. A critical investigation of the effect of hygrothermal cycling on hydration and in-plane/through-plane proton conductivity of Nafion 117 at medium temperature (70-130 C). *J Power Sources* **2013**,235, 129-134.
- [13]. Yadav,R.; Fedkiw. P. S.; Analysis of EIS Technique and Nafion 117 Conductivity as a Function of Temperature and Relative Humidity. *J. Electrochem. Soc.* **2012**,159 (3), B340-B346.
- [14]. Cooper, K. R. Characterizing Through-Plane and In-Plane Ionic Conductivity of Polymer Electrolyte Membranes. *ECS Transactions* **2011**,41 (1), 1371-1380.
- [15]. Jiang, R.; Mittelsteadt, C. K.; Gittleman,C. S. Through-Plane Proton Transport Resistance of Membrane and Ohmic Resistance Distribution in Fuel Cells. *J. Electrochem. Soc.* **2009**,156(12), B1440-B1446.
- [16]. Mu ´ ller, F.; Ferreira, C. A.; Azambuja, D. S. et al. Measuring the Proton Conductivity of Ion-Exchange Membranes Using Electrochemical Impedance Spectroscopy and Through-Plane Cell. *J. Phys. Chem. B* **2014**, 118, 1102–1112.
- [17]. Heimerdinger, P.; Rosin, A.; Danzer, M. A.; et al. A Novel Method for Humidity-Dependent Through-Plane Impedance Measurement for Proton Conducting Polymer Membranes. *Membranes* **2019**, 9, 62.
- [18]. Soboleva,T.; Xie, Z.; Shi,Z. et al. Investigation of the through-plane impedance technique for evaluation of anisotropy of proton conducting polymer membranes. *J. Electroanal. Chem.* **2008**, 622,145–152.
- [19]. Al-Madani, G.; Kailani, M. H.; Al-Hussein. M.; Test System For Through-Plane Conductivity Measurements of Hydrogen Proton Exchange Membranes. *Int. J. Electrochem. Sci.* **2015**,10, 6465 – 6474
- [20]. Kim,Y. S.; Lee, K.S. Fuel Cell Membrane Characterizations. *Polymer Reviews* **2015**, 55(2) 330-370.
- [21]. Peron, J.; Mani, A.; Zhao, X.; et al.Properties of Nafion® NR-211 membranes for PEMFCs. *J. Membrane Sci.* **2010**,356,44–51.
- [22]. Schalenbach, M.; Lueke, W.; Lehnert,W.; et al.The influence of water channel geometry and proton mobility on the conductivity of Nafion®. *Electrochim. Acta* **2016**,214, 362–369.
- [23]. Jin, F.; Yan, K.; Zhao, Y.; et al. Surface Enriched Sulfonic Acid Ionic Clusters of Nafion Nanofibers as Long-Range Interconnected Ionic Nanochannels for Anisotropic Proton Transportation: Phenomenon and Molecular Mechanism. *Adv.*

-
- Mater. Interfaces* **2020**, 7, 2000342.
- [24]. Alberti, G.; Narducci, R.; Vona, M. L. D.; et al. More on Nafion Conductivity Decay at Temperatures Higher than 80 °C: Preparation and First Characterization of In-Plane Oriented Layered Morphologies. *Ind. Eng. Chem. Res.* **2013**, 52, 10418–10424.
- [25]. Ekdunge, Y. S.; Simonsson, D. Proton Conductivity of Nafion 117 as Measured by a Four-Electrode AC Impedance Method. *J. Electrochem. Soc.* **1996**, 143(4), 1254-1259.
- [26]. DeCaluwe, S. C.; Baker, A. M.; Bhargava, P.; et al. Structure-property relationships at Nafion thin-film interfaces: Thickness effects on hydration and anisotropic ion transport. *Nano Energy* **2018**, 46, 91–100.
- [27]. Schwämmlein, J. N.; Pham, N. L. T.; Mittermeier, T.; et al. Through-Plane Conductivity of Anion Exchange Membranes at Sub-Freezing Temperatures—Hydroxide vs (Bi-)Carbonate Ions. *J. Electrochem. Soc.* **2020**, 167, 084513.
- [28]. Matos, B.R. The genuine ac-to-dc proton conductivity crossover of nafion and polymer dielectric relaxations as a fuel cell polarization loss. *J. Electroanal. Chem.* **2020**, 871, 114357.
- [29]. Jash, P.; Parashar, R. K.; Fontanesi, C.; et al. The Importance of Electrical Impedance Spectroscopy and Equivalent Circuit Analysis on Nanoscale Molecular Electronic Devices. *Adv. Funct. Mater.* **2022**, 32, 2109956.
- [30]. Amphlett, J. C.; Baumert, R. M.; Mann, R. F.; et al. Performance Modeling of the Ballard Mark IV Solid Polymer Electrolyte Fuel Cell. I. Mechanistic Model Development. *J. Electrochem. Soc.* **1995**, 142(1), 1-8.
- [31]. Kamel, M. S. A.; Mohamed, H. F. M.; M. O.; et al. Characterization and evaluation of Nafion HP JP as proton exchange membrane: transport properties, nanostructure, morphology, and cell performance. *J. Solid State Electrochemistry*, **2019**, 23:2639–2656.
- [32]. Schneider, I. A.; Bayer, M. H.; Wokaun, A.; et al. Impedance Response of the Proton Exchange Membrane in Polymer Electrolyte Fuel Cells. *J. Electrochem. Soc.* **2008**, 155(8), B783-B792.
- [33]. Futter, G. A.; Gazdzicki, P.; Friedrich, K. A.; et al. Physical modeling of polymer-electrolyte membrane fuel cells: Understanding water management and impedance spectra. *J. Power Sources* **2018**, 391, 148–161.
- [34]. Gerling, C.; Hanauer, M.; Berner, U.; et al. Experimental and Numerical Investigation of the Low-Frequency Inductive Features in Differential PEMFCs: Ionomer Humidification and Platinum Oxide Effects. *J. Electrochem. Soc.* **2023**, 170 014504.
- [35]. Cruz-Manzo, S.; Greenwood, P. Low Frequency Inductive Loop in EIS Measurements of an Open-Cathode Polymer Electrolyte Fuel Cell Stack. Impedance of Water Vapour Diffusion in the Cathode Catalyst Layer. *J. Electroanalytical Chemistry*, **2021**, <https://doi.org/10.1016/j.jelechem.2021.115733>.
- [36]. Cruz-Manzo, S.; Perezmitre-Cruz, U.; Greenwood, P.; et al. An impedance model for Analysis of EIS of Polymer Electrolyte Fuel Cells under Platinum

- Oxidation and Hydrogen Peroxide Formation in the Cathode. *J. Electroanaly. Chem.* 2016, 771, 94-105.
- [37]. Cruz-Manzo, S.; Cano-Castillo, U.; Greenwood, P. Impedance Study on Estimating Electrochemical Mechanisms in a Polymer Electrolyte Fuel Cell During Gradual Water Accumulation. *Fuel Cells* **2019**, 19(1), 71–83..
- [38]. Meyer, Q.; Liu, SY.; Ching, KR.; et al. Operando monitoring of the evolution of triple-phase boundaries in proton exchange membrane fuel cells. *J. Power sources*. DOI10.1016/j.jpowsour.2022.232539
- [39]. Zhang, W.; Ma, J.; Wang, P.; et al. Investigations on the interfacial capacitance and the diffusion boundary layer thickness of ion exchange membrane using electrochemical impedance spectroscopy. *J. Membrane Sci.* **2016**, 502, 37–47.
- [40]. Mohamed, H. F. M.; Kobayashi, Y.; Kuroda, C. S.; et al. Impact of Heating on the Structure of Perfluorinated Polymer Electrolyte Membranes: A Positron Annihilation Study. *Macromol. Chem. Phys.* **2011**, 212, 708–714.
- [41]. Cao, C.N.; Zhang, J.Q. An Introduction to Electrochemical Impedance Spectroscopy. *Science Press*, Beijing, **2002**.
- [42]. Mohamed, H. F. M.; Kobayashi, Y.; Kuroda, C. S.; et al. Effects of Ion Exchange on the Free Volume and Oxygen Permeation in Nafion for Fuel Cells. *J. Phys. Chem. B.* **2009**, 113, 2247–2252.
- [43]. Mohamed, H. F. M.; Kobayashi, Y.; Kuroda, C. S.; et al. Positron annihilation study of ion-exchanged forms of Nafion® membrane, *Phys. Status Solidi C.* **2009**, 6(11), 2392–2396.
- [44]. Mohamed, H. F.M.; Abdel-Hady, E.E.; Abdel-Hamed, M.O.; et al. Microstructure Characterization of Nafion® HP JP as a Proton Exchange Membrane for Fuel Cell: Positron Annihilation Study. *Acta Phys. Pol. A* **2017**, 132(5), 1543-1547.
- [45]. Olesen, A. C.; Berning, T.; Kær, S. K. On the Diffusion Coefficient of Water in Polymer Electrolyte Membranes. *ECS Transactions*, **2013**, 50(2), 979-991.
- [46]. Luo, X.; Lau, G.; Tesfaye, M.; et al. Thickness Dependence of Proton-Exchange-Membrane Properties. *J. Electrochem. Soc.* **2021**, 168, 104517.
- [47]. Shimpalee, S.; Lilavivat, V.; Xu, H.; et al. The Effect of Membrane Properties on Performance and Transports inside Polymer Electrolyte Membrane Fuel Cells. *J. Electrochem. Soc.* **2018**, 165(11), F1019-F1026.
- [48]. Lufrano, E.; Simari, C.; Vona, M. L. D.; et al. How the Morphology of Nafion-Based Membranes Affects Proton Transport. *Polymers* **2021**, 13, 359-11.
- [49]. Ohira, A.; Kuroda, S.; Mohamedz H. F. M.; et al. Effect of interface on surface morphology and proton conduction of polymer electrolyte thin films. *Phys. Chem. Chem. Phys.*, **2013**, 15, 11494-11500.
- [50]. Zhu, Y.; Ding, L.; Liang, X.; et al. Beneficial use of rotatable-spacer side-chains in alkaline anion exchange membranes for fuel cells. *Energy Environ. Sci.*, **2018**, 11, 3472-3479.
- [51]. He, Y.; Si, J.; Wu, L.; et al. Dual-cation comb-shaped anion exchange membranes: Structure, morphology and properties. *J. Membrane Sci.* **2016**, 515, 189–195.

-
- [52]. Peron, J.; Mani, A.; Zhao, X. et al. Properties of Nafion® NR-211 membranes for PEMFCs. *J. Membrane Sci.* **2010**, *356*,44–51.
- [53]. Jash,P.; Parashar, R. K.; Fontanesi, C.; et al. The Importance of Electrical Impedance Spectroscopy and Equivalent Circuit Analysis on Nanoscale Molecular Electronic Devices. *Adv. Funct. Mater.* **2022**, *32*, 2109956
- [54]. Pivac,I.; Simi, B.; Barbir. F. Experimental diagnostics and modeling of inductive phenomena at low frequencies in impedance spectra of proton exchange membrane fuel cells. *J. Power Sources* **2017** ,*365* ,240-248.
- [55]. Karden, E.; Buller, S.; Doncker. R. W. D. A frequency-domain approach to dynamical modeling of electrochemical power sources. *Electrochim. Acta* **2002**, *47*, 2347-2356.
- [56]. Thapa, A.; Gao, H. Low-frequency Inductive Loop and Its Origin in the Impedance Spectrum of a Graphite Anode, *J. Electrochemi. Soc.* **2022**,DOI10.1149/1945-7111/aca364
- [57]. Liang, X.W.; Su, Y.H. ; Yang,T.S. et al. Effect of Ti Addition on the Microstructure and Corrosion Resistance of AlCrCuFeNiNb0.2 High-Entropy Alloy. *JOM* **2023**,*75*(2), 428-436.
- [58]. Liu, D. Q. ; Blackwood, D. J. An EIS Investigation into the Influence of HF Concentration on Porous Silicon Formation, *J. Electrochemi. Soc.* **2014**,*161* (3) ,E44-E52.
- [59]. Chen, Z.; Luo,S.; Yao, L.; et al .The inductive effect of montmorillonite/polyether sulfone membrane during the ion diffusion process. *Applied Clay Science* **2021**, *203*, 106002.

Table 1 The fitted parameters from equivalent circuit for EIS in 1st day

param	R ₀	CPE-Y ₀ (ohm ⁻¹	CPE-n	R ₁	R ₂	L ₂	Chi-square
eters	(ohm)	cm ² s ⁻ⁿ)		(ohm)	(ohm)	(Henry)	
20 °C	-12.73	6.7*10 ⁻¹⁰	0.9738	1402	18257	22.52	0.4253
30 °C	0.8548	4.99*10 ⁻¹⁰	0.9965	1342	4407	68.82	0.0322
40 °C	5.029	6.05*10 ⁻¹⁰	0.9825	1153	6656	1676	0.0202
50 °C	5.742	6.71*10 ⁻¹⁰	0.9759	966	6275	1024	0.0283
60 °C	13.87	6.23*10 ⁻¹⁰	0.9823	800	8514	2292	0.0863
70 °C	20.24	7.19*10 ⁻⁹	0.9779	662	6323	647	0.0399
80 °C	15.58	1.72*10 ⁻⁹	0.9253	572	3454	364.2	0.0374
90 °C	11.99	2.23*10 ⁻⁹	0.9123	514	3006	158	0.0267
100 °C	15.18	1.71*10 ⁻⁹	0.9329	455	1645	670	0.0520

(J.W. GUO et al.)

Table 2 The fitted parameters from equivalent circuit for EIS in 2nd day

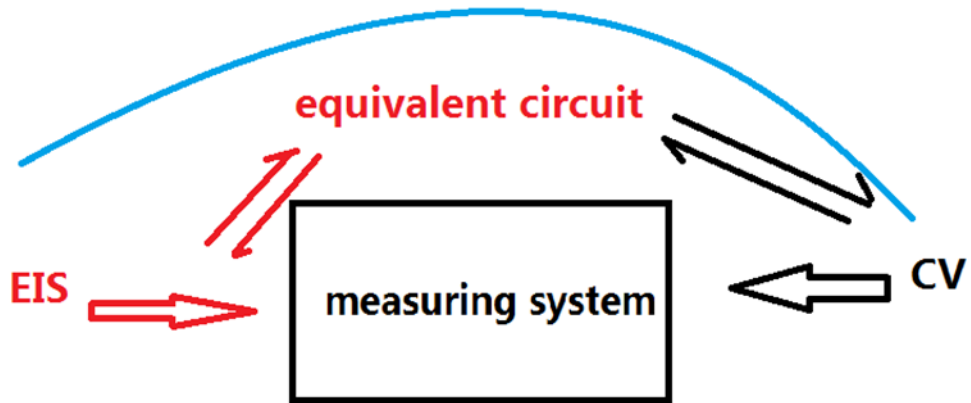
param	R ₀	CPE-Y ₀	CPE-n	R ₁	R ₂	L ₂	Chi-
eters	(ohm)	(ohm ⁻¹ cm ⁻² s ⁻ⁿ)		(ohm)	(ohm)	(Henry)	square
20 °C	4.209	1.95*10 ⁻⁹	0.9209	1224	3660	3508	0.009
30 °C	-15.9	2.94*10 ⁻⁹	0.8903	1202	8108	8180	0.056
40 °C	5.111	2.24*10 ⁻⁹	0.9133	979	7579	3723	0.039
50 °C	19.01	1.91*10 ⁻⁹	0.9250	844	4621	3014	0.007
60 °C	14.03	1.95*10 ⁻⁹	0.9223	752	4130	4110	0.010
70 °C	-4.96	2.64*10 ⁻⁹	0.8957	707	4175	2036	0.011
80 °C	15.58	1.56*10 ⁻⁹	0.9404	642	2318	709	0.015
90 °C	12.51	1.78*10 ⁻⁹	0.9304	596	2582	287	0.026
100 °C	14.90	1.96*10 ⁻⁹	0.9226	538	1625	698	0.038

(J.W. GUO et al.)

Table 3 The fitted parameters from equivalent circuit for EIS in 3rd day

param	R ₀	CPE-Y ₀ (ohm ⁻¹ cm ² s ⁻ⁿ)	CPE-n	R ₁	R ₂	L ₂	Chi-
eters	(ohm)			(ohm)	(ohm)	(Henry)	square
20 °C	18.1	2.12*10 ⁻⁹	0.9268	1419	5922	3052	0.0316
30 °C	31.08	2.00*10 ⁻⁹	0.9345	1356	4786	1739	0.0250
40 °C	20.96	1.90*10 ⁻⁹	0.9361	1205	4687	793	0.0224
50 °C	32.36	1.91*10 ⁻⁹	0.9378	1025	4219	946	0.0205
60 °C	20.50	3.05*10 ⁻⁹	0.8979	905	5288	638	0.0210
70 °C	18.46	2.13*10 ⁻⁹	0.9143	777	4401	715	0.0123
80 °C	6.876	2.47*10 ⁻⁹	0.8977	712	5224	674	0.0100
90 °C	11.84	2.30*10 ⁻⁹	0.9028	641	3796	1199	0.0100
100 °C	5.52	3.22*10 ⁻⁹	0.8816	611	4598	856	0.0074

(J.W. GUO et al.)



Scheme. The proposed study scheme in this work

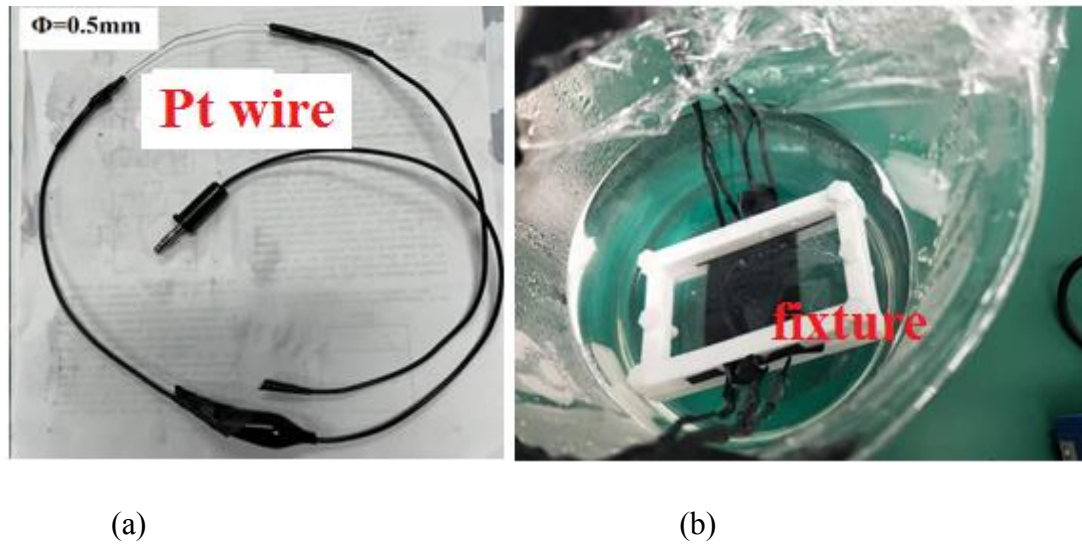
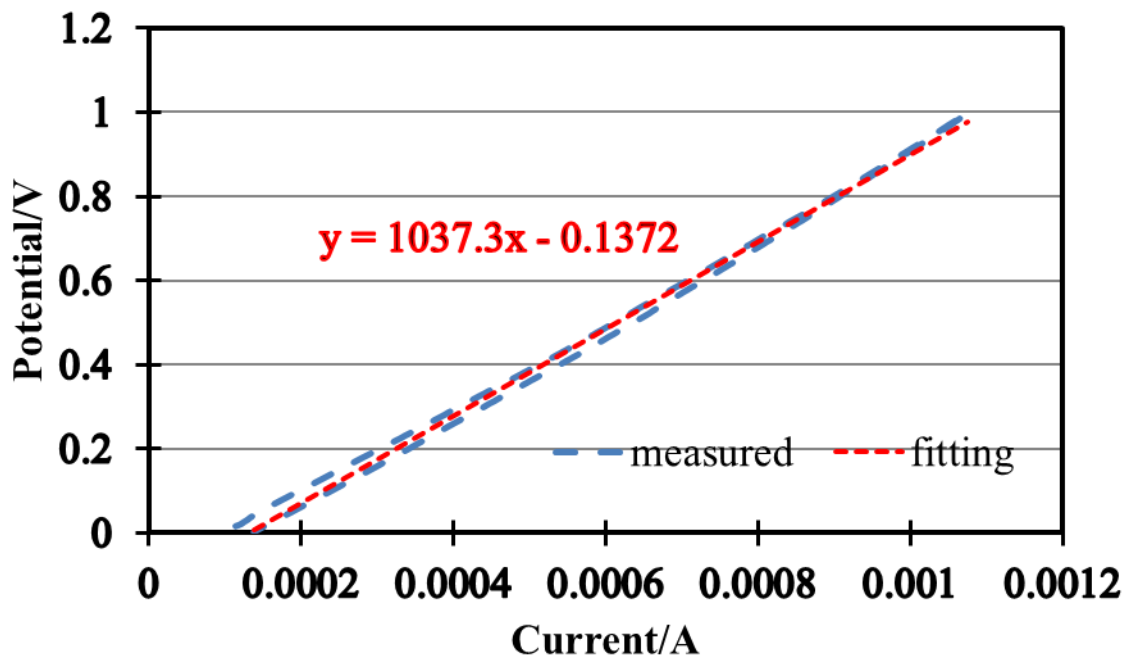
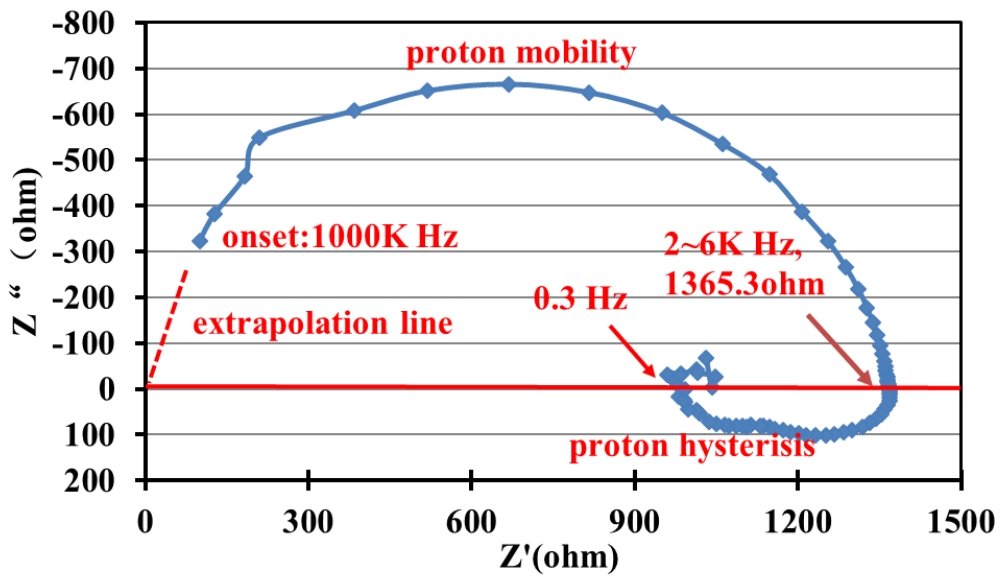


Fig.1 The illustration for in-plane conductivity measurement; (a) Pt wire electrode, (b)The fixture with Nafion membrane, (c) The electrode and Nafion membrane composition, where d is current line distance (1cm), w and t are membrane length(5cm) and thickness ($27.5\ \mu\text{m}$)

(J.W. GUO et al.)



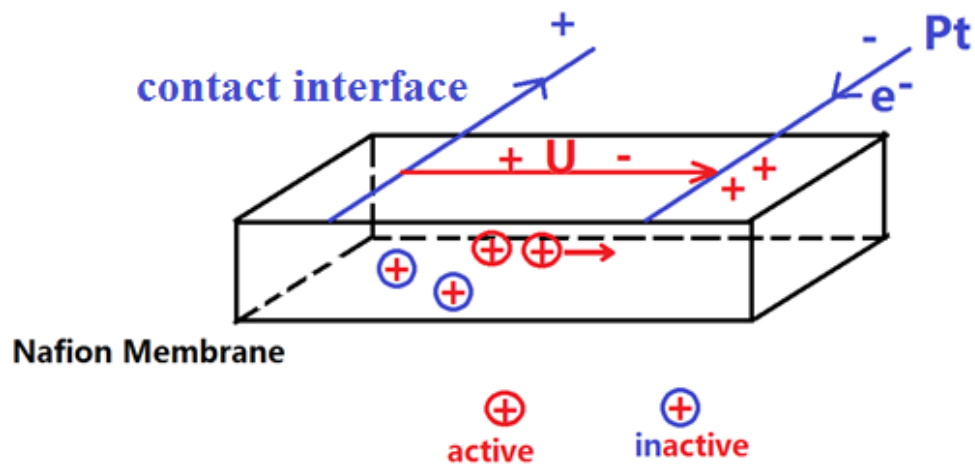
(a)



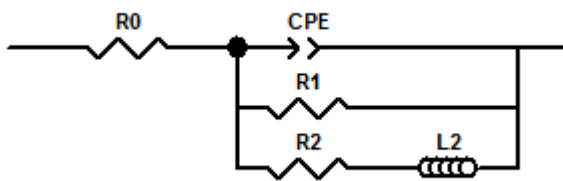
(b)

Fig.2 The in-plane measurement for Nafion membrane at 30 °C condition, 1st day: (a) CV plot, (b) Nyquist plot in EIS measurement.

(J.W. GUO et al.)



(a)

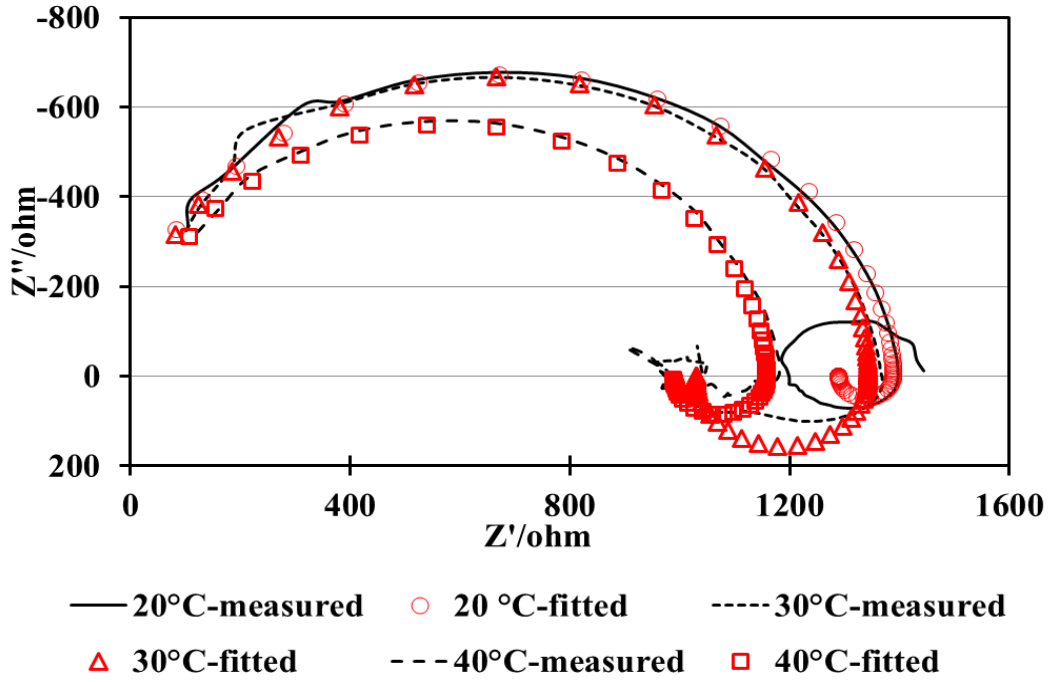


(b)

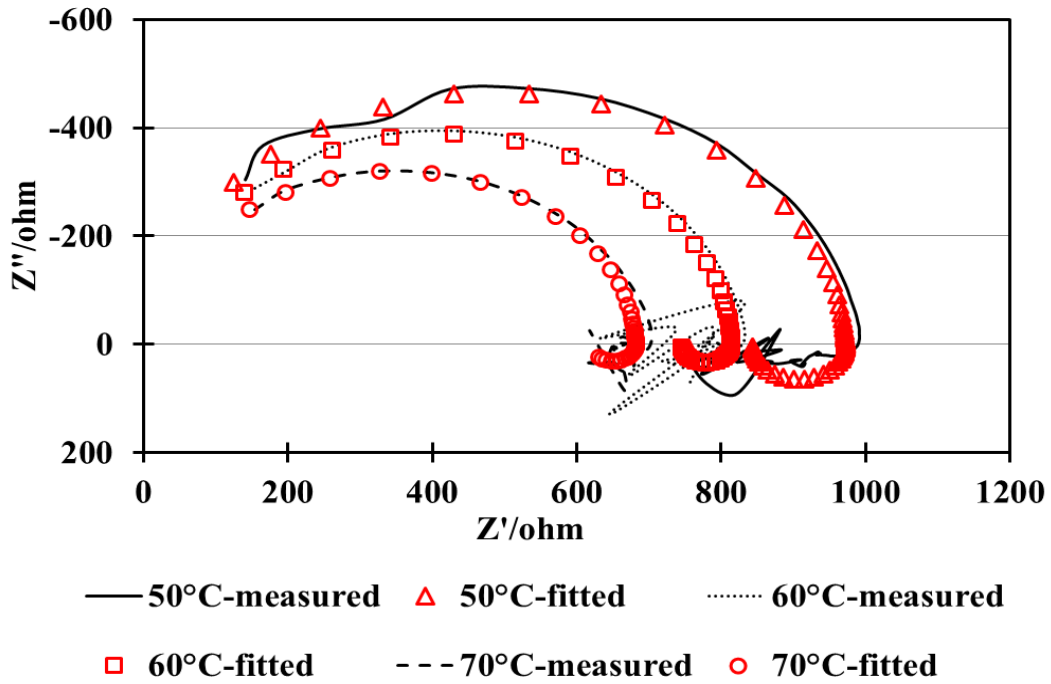
Fig.3 (a)The measurement under both DC and AC approaches.

(b)The proposed equivalent circuit

(J.W. GUO et al.)

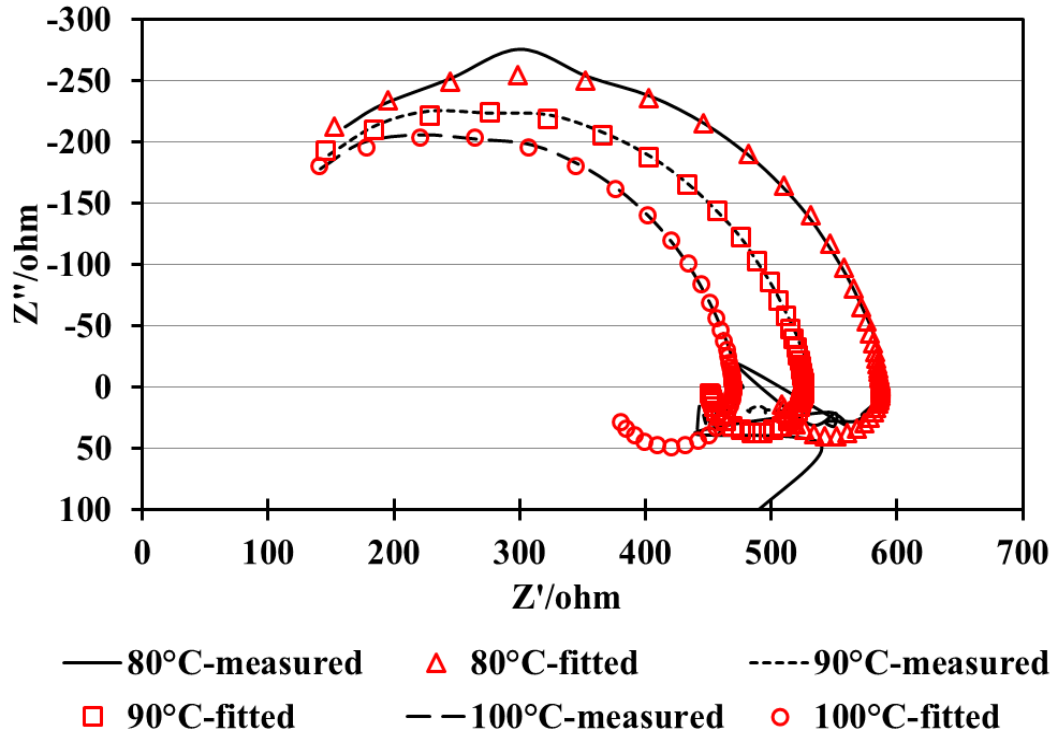


(a)



(b)

(J.W. GUO et al.)

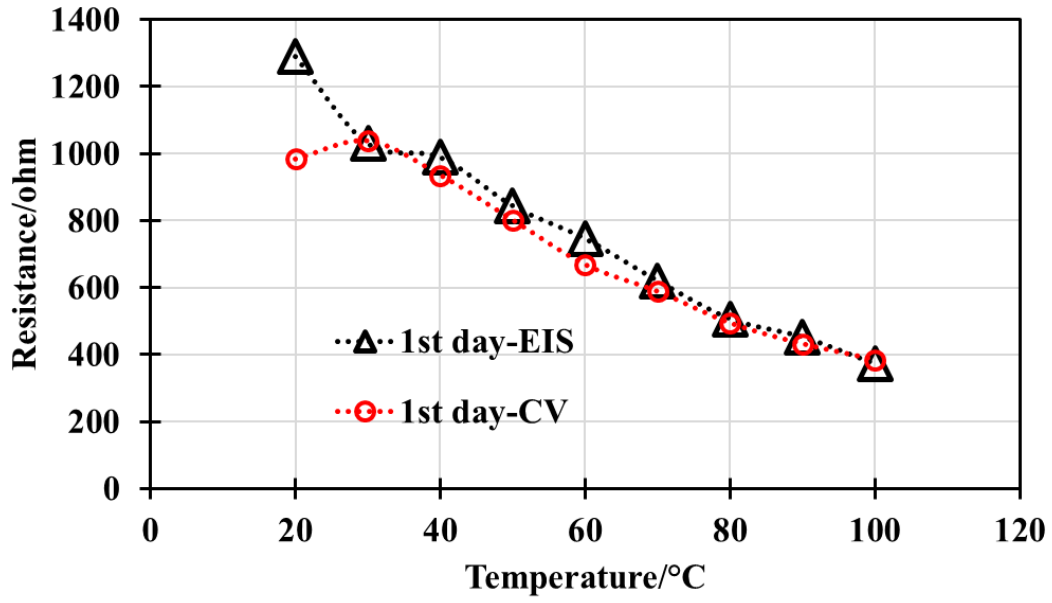


(c)

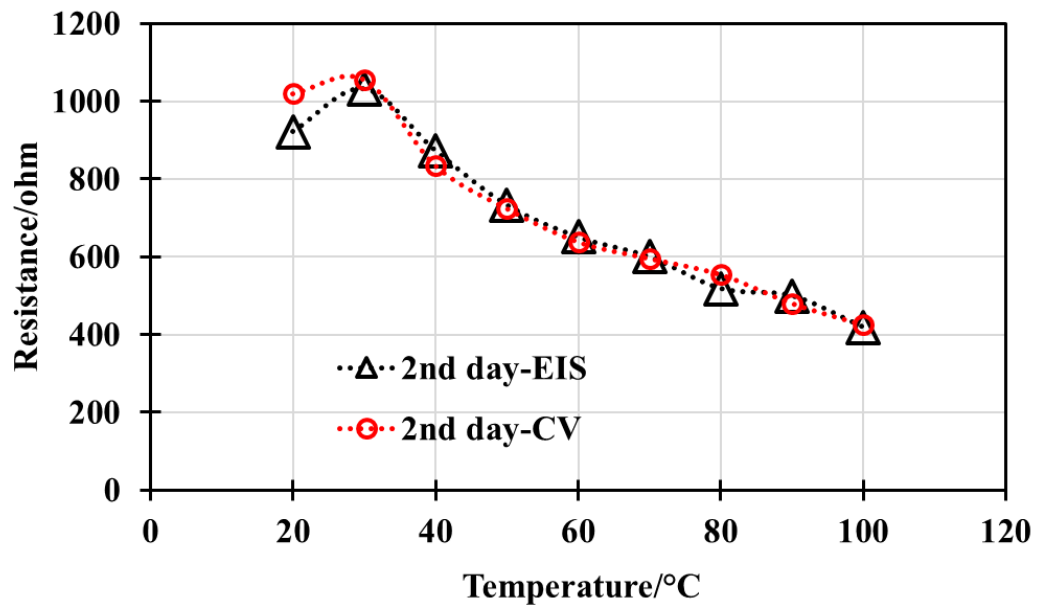
Fig.4 The temperature effect on measured and fitted Nyquist spectrum in 1st day. (a)

20-40 °C; (b)50-70 °C;(c) 80-100 °C.

(J.W. GUO et al.)

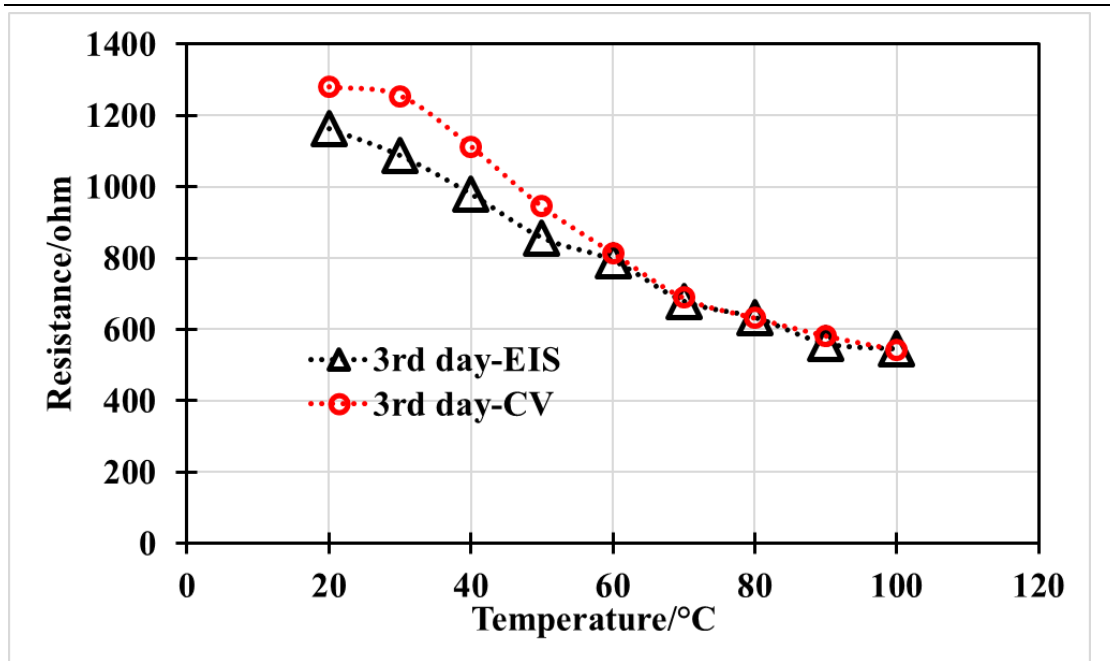


(a)



(b)

(J.W. GUO et al.)



(c)

Fig.5 The comparison for the measured resistance in CV measurement and the fitted resistance of $R_0 + R_1 R_2 / (R_1 + R_2)$ from EIS measurement under successive temperature cycles. (a) 1st day; (b) 2nd day; (c) 3rd day.

(J.W. GUO et al.)

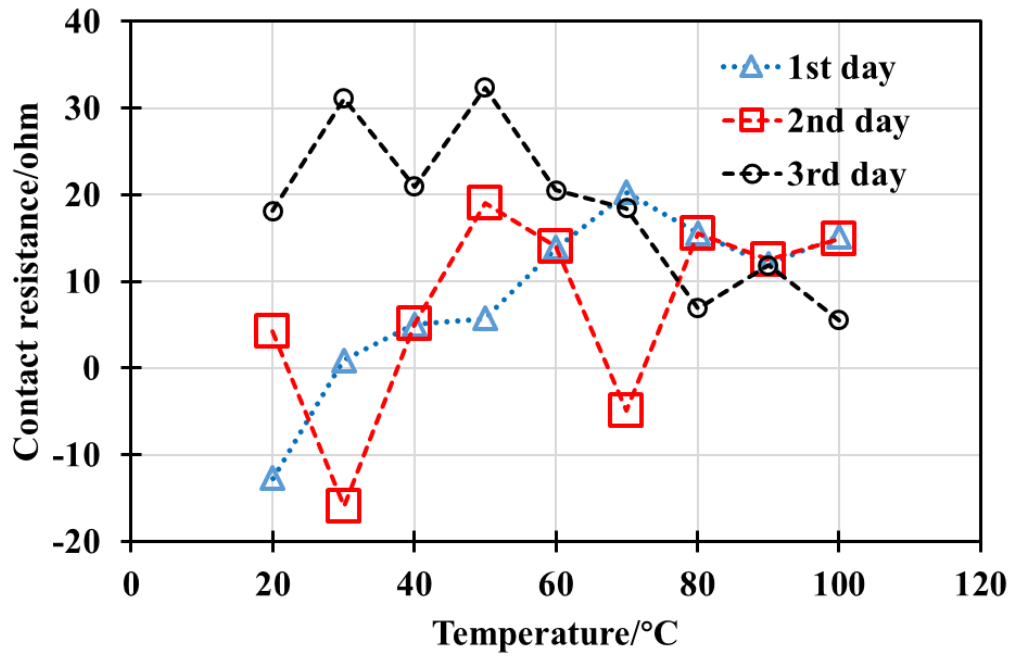
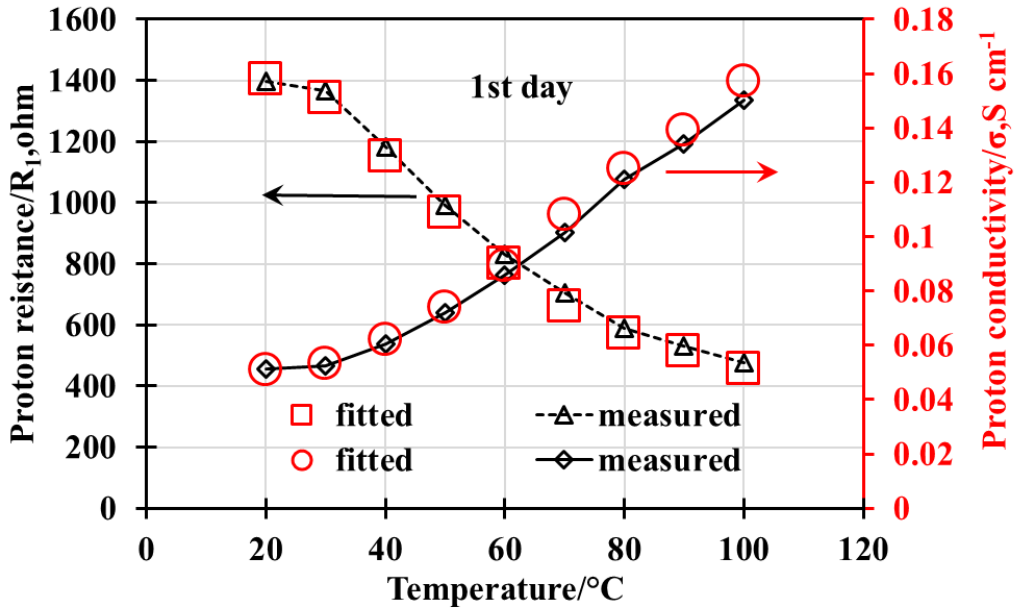
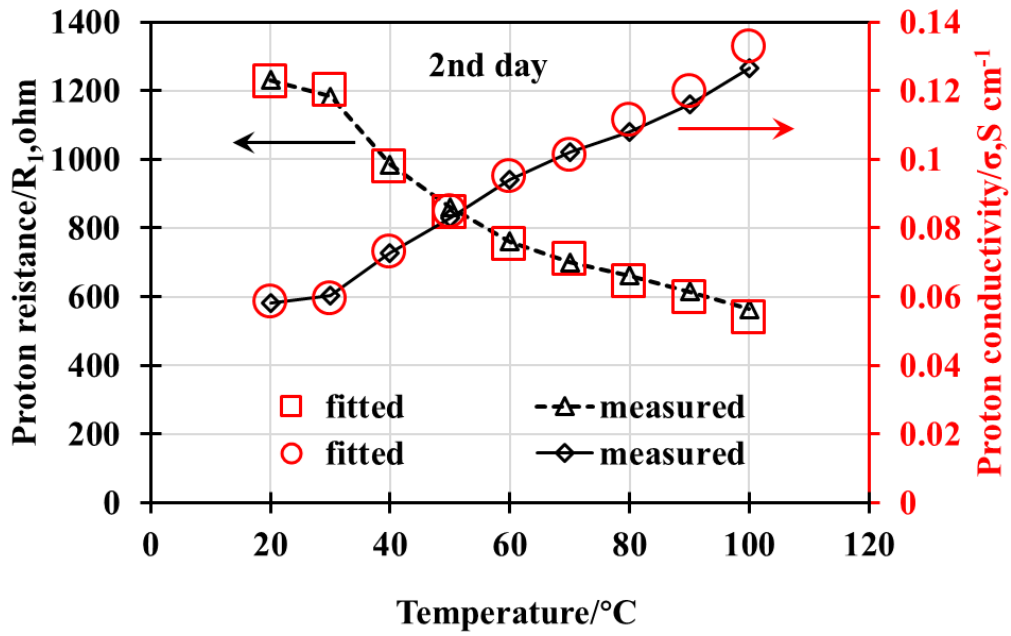


Fig. 6 The contact resistance(R_0) under the successive temperature cycles

(J.W. GUO et al.)

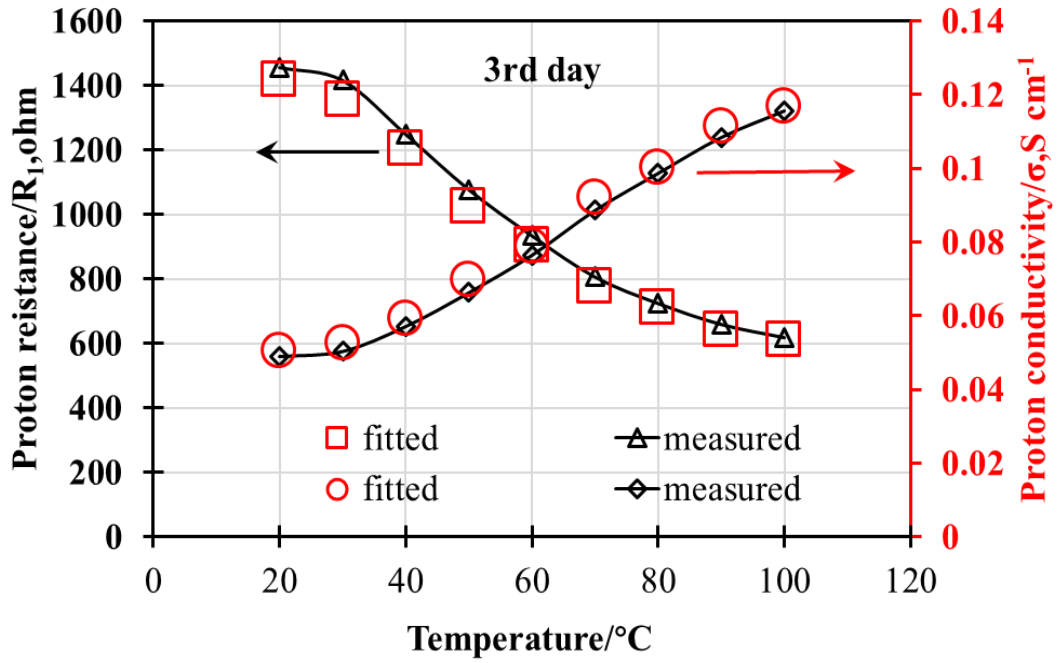


(a)



(b)

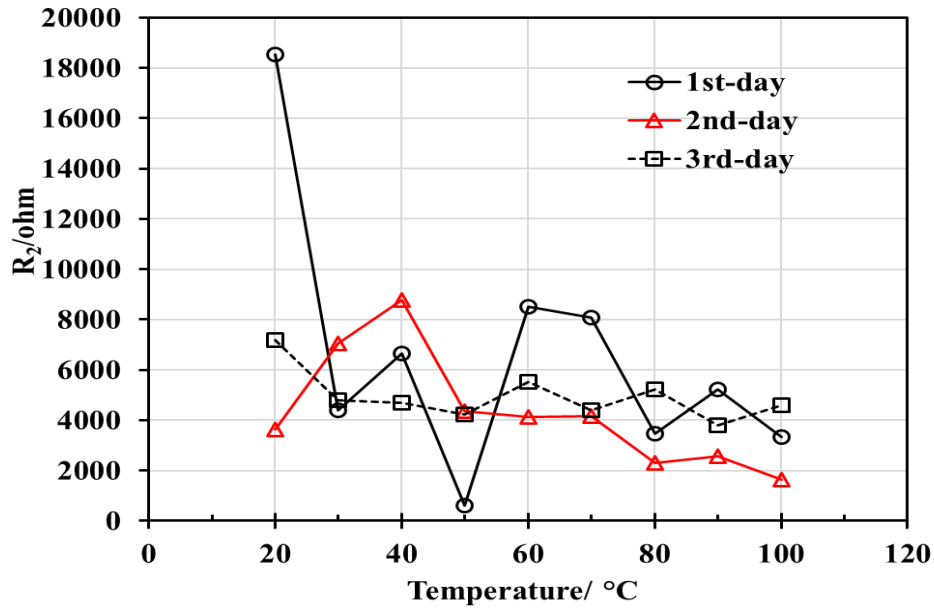
(J.W. GUO et al.)



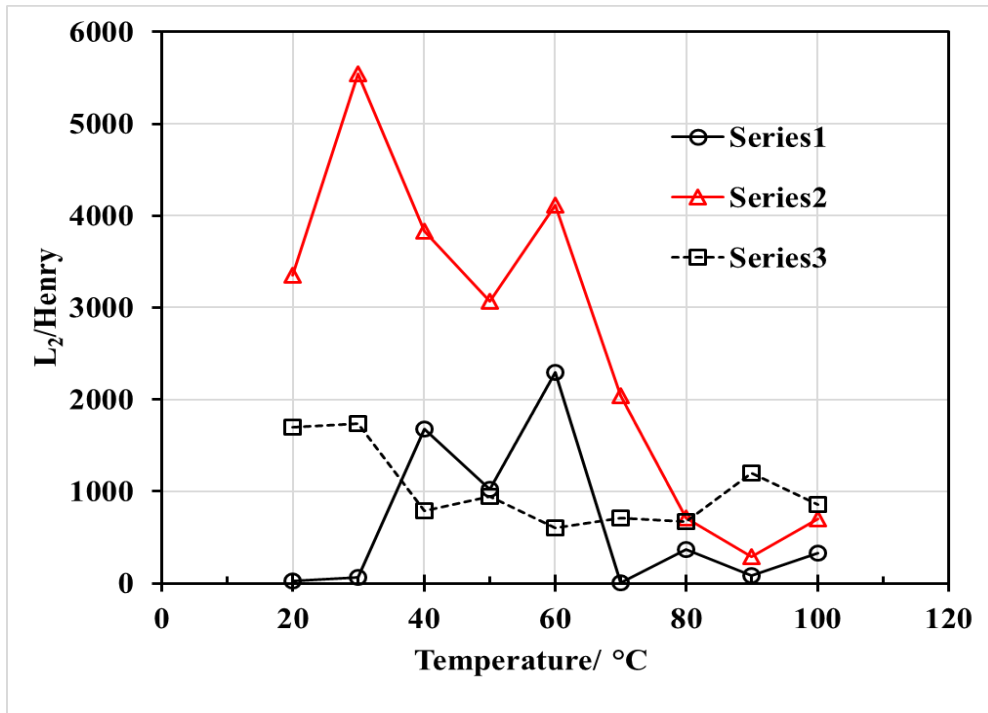
(c)

Fig.7 The measured (2-6K Hz) and fitted proton resistances(R_1 , ohm), proton conductivity (σ , $S\ cm^{-1}$) under successive temperature cycles. (a) 1st day. (b) 2nd day; (c)3rd day

(J.W. GUO et al.)



(a)



(b)

Fig.8 The effect of successive temperature cycles on the water hysteresis in Nafion membrane. (a)The resistances(R_2). (b) the inductance(L_2)

(J.W. GUO et al.)